Clinical and Translational Radiation Oncology 42 (2023) 100663

Contents lists available at ScienceDirect

Clinical and Translational Radiation Oncology

journal homepage: www.sciencedirect.com/journal/clinical-and-translational-radiation-oncology

A total inverse planning paradigm: Prospective clinical trial evaluating the performance of a novel MR-based 3D-printed head immobilization device

Paola Anna Jablonska [a,b,c,1], Amy Parent [b,1], Nancy La Macchia [b,1], Harley H.L. Chan [d,1], Matthew Filleti [b], Matthew Ramotar [b], Young-Bin Cho [a,b,e], Maria Braganza [b], Adam Badzynski [f], Normand Laperriere [a,b], Tatiana Conrad [a,b], Derek S. Tsang [a,b], David Shultz [a,b], Anna Santiago [b,g], Jonathan C. Irish [d,h], Barbara-Ann Millar [a,b], Tony Tadic [a,b,d,1,2], Alejandro Berlin [a,b,d,f,*,1,2]

[a] *Department of Radiation Oncology, University of Toronto, 149 College Street, Unit 504, Toronto, Ontario M5T 1P5, Canada*
[b] *Radiation Medicine Program, Princess Margaret Cancer Centre, University Health Network, 700 University Avenue, 7th Floor, Toronto, Ontario M5G 1Z5, Canada*
[c] *Department of Radiation Oncology, Clinica Universidad de Navarra, 31008 Pamplona, Spain*
[d] *Guided Therapeutics (GTx) Program, Techna Institute, University Health Network, University of Toronto, 200 Elizabeth Street, Toronto, Ontario M5G 2C4, Canada*
[e] *Department of Radiation Oncology, Cleveland Clinic, 9500 Euclid Avenue, Cleveland, OH 44195, USA*
[f] *Cancer Digital Intelligence Program, Princess Margaret Cancer Centre, University Health Network, 700 University Avenue, 7th Floor, Toronto, Ontario M5G 1Z5, Canada*
[g] *Department of Biostatistics, Princess Margaret Cancer Centre, University Health Network, 610 University Avenue, Toronto, Ontario M5G 2M9, Canada*
[h] *Department of Otolaryngology – Head and Neck Surgery/Surgical Oncology, Princess Margaret Cancer Centre/University Health Network, 610 University Avenue, Toronto, Ontario M5G 2M9, Canada*

ARTICLE INFO

Keywords:
3D printing
Radiotherapy
MR-guidance
Mask
Immobilization device

ABSTRACT

Background and purpose: Brain radiotherapy (cnsRT) requires reproducible positioning and immobilization, attained through redundant dedicated imaging studies and a bespoke moulding session to create a thermoplastic mask (T-mask). Innovative approaches may improve the value of care. We prospectively deployed and assessed the performance of a patient-specific 3D-printed mask (3Dp-mask), generated solely from MR imaging, to replicate a reproducible positioning and tolerable immobilization for patients undergoing cnsRT.

Material and methods: Patients undergoing LINAC-based cnsRT (primary tumors or resected metastases) were enrolled into two arms: control (T-mask) and investigational (3Dp-mask). For the latter, an in-house designed 3Dp-mask was generated from MR images to recreate the head positioning during MR acquisition and allow coupling with the LINAC tabletop. Differences in inter-fraction motion were compared between both arms. Tolerability was assessed using patient-reported questionnaires at various time points.

Results: Between January 2020 - July 2022, forty patients were enrolled (20 per arm). All participants completed the prescribed cnsRT and study evaluations. Average 3Dp-mask design and printing completion time was 36 h:50 min (range 12 h:56 min – 42 h:01 min). Inter-fraction motion analyses showed three-axis displacements comparable to the acceptable tolerance for the current standard-of-care. No differences in patient-reported tolerability were seen at baseline. During the last week of cnsRT, 3Dp-mask resulted in significantly lower facial and cervical discomfort and patients subjectively reported less pressure and confinement sensation when compared to the T-mask. No adverse events were observed.

Conclusion: The proposed total inverse planning paradigm using a 3D-printed immobilization device is feasible and renders comparable inter-fraction performance while offering a better patient experience, potentially improving cnsRT workflows and its cost-effectiveness.

* Corresponding author at: Department of Radiation Oncology, University of Toronto, 149 College Street, Unit 504, Toronto, Ontario M5T 1P5, Canada.
E-mail address: alejandro.berlin@rmp.uhn.ca (A. Berlin).
[1] These authors contributed equally.
[2] Co-senior authors.

https://doi.org/10.1016/j.ctro.2023.100663
Received 9 May 2023; Received in revised form 25 June 2023; Accepted 20 July 2023
Available online 26 July 2023

1. Introduction

Brain radiotherapy (RT) is an integral treatment for most primary brain tumors and a significant proportion (e.g., 10–30%) of all cancer patients [1]. Diagnosis and referral for brain RT is often based on a magnetic resonance (MR). Nevertheless, RT planning requires additional imaging procedures (i.e., computed tomography (CT) 'simulation' [CT-sim]). Prior to CT-sim acquisition, a moulding session takes place in which a thermoplastic mask [T-mask] is customized to achieve a reference head positioning during CT-sim that is reproduced during RT delivery sessions. However, available, or new MR image sets are still required and registered to the CT-Sim for best delineation of tumor and critical structures. Traditionally, CT was essential for RT dose calculation, but robust MR-based methods have emerged [2]. Hence, the residual indispensability of CT-sim and its moulding session pertain to the attainment of a reproducible positioning and immobilization during RT planning and delivery.

Additive manufacturing (i.e., 3D-printing) is increasingly used across many nonmedical fields [3]. New medical applications have emerged in domains such as education, research, surgical planning, instrumentation, implants, and prostheses [4]. In RT, 3D-printing has been used for generating custom dose modulation boluses [5], oral retractors [6] and brachytherapy applicators [7]. Growing use-cases of 3D-printing technologies pave the way for greater availability and affordability, while supporting its safety in the clinical setting.

We sought to capitalize on additive manufacturing to reimagine the current brain RT workflow. The CT-sim and T-mask *status quo* calls for additional visits, potential delays, discomfort, and anxiety in one every four of patients [8]. We hypothesized that head positioning during MR could be accurately recreated, non-invasively immobilized, and robustly reproduced using a 3D-printed mask (3Dp-mask). If true, the entire brain RT planning process would necessitate solely an MR image-set, in turn making moulding session, additional imaging and/or image registration superfluous. As a result, a novel 'total inverse planning' paradigm would emerge, streamlining patient's experience and RT department human and imaging resource allocation.

2. Materials & methods

This is an investigator-initiated, single-institution, open-label, two-arm, IRB-approved registered study (#18-5753, NCT04114786; Supplementary Materials). All participants provided written informed consent. Eligible patients were $\geq$ 18 years old with diagnosis of brain tumour (primary or resected metastases), considered for photon LINAC-based radical or adjuvant RT in $\geq$ 5 fractions, without contraindications to MR.

2.1. RT simulation and planning

The study had two arms, control (i.e., treatment with T-mask) and investigational (i.e., treatment with 3Dp-mask). Allocation was based on the patient's preference. All participants underwent MR (3.0-T Verio; Siemens Medical Systems, Erlangen, Germany) and CT-sim including T-mask moulding session (three-point head mask; Orfit Industries, Wijnegem, Belgium) as per Institutional standard-of-care. Patients in the investigational arm underwent a second CT-sim with their manufactured 3Dp-mask. MR images were acquired with a 3 T Siemens Skyra Fit 20-channel head and neck coil, applying a field-of-view [FOV] 20 cm, in-plane resolution 0.6 $\times$ 0.6 $\times$ 1.5 mm thickness reconstructions, 0.75 mm overlap. The FOV were tailored to ensure the entire head surface up to C1/C2 vertebral bodies caudally and the nasal bridge (or the entire nose) were encompassed to allow most adequate fit of the 3Dp-mask. 3D MPRage T1-weighted contrast-enhanced (repetition time [TR], 1400 ms; echo time [TE], 2.2 ms, matrix 320x320, Bw 400 Hz/Px) and T2-weighted turbo spin echo (TSE; TR 4850 ms; TE, 105 ms, matrix 384x384, Bw 224 Hz/Px) sequences were included.

In the control arm, the MR was rigidly registered to the CT-sim which was used for plan calculation purposes (RayStation 8B; RaySearch Laboratories, Stockholm, Sweden). In the investigational arm, the second CT-sim with the 3Dp-mask was acquired and used for RT planning, as the evaluation of RT planning using MR-inferred densities has been previously studied and was not a primary objective of this work. In addition, the first CT-sim (i.e., with T-mask) was warped and registered to the MR with the intention to limit eventual delays by allowing preliminary RT planning while the 3Dp-mask was being created. Also, the original CT-sim and T-mask were kept as back-up in case of any unforeseen circumstances during RT planning, quality-assurance, or delivery. Finally, the two CT-sim sets permitted additional verifications and quantitative ascertainments of the investigational workflow during this proof-of-concept study: i) confirming accuracy of the patient positioning with the 3Dp-mask (i.e., displacements $\leq$ 3 mm to reference MR and warped CT); ii) transfer of an intact (i.e. non-warped) image set to the treatment units for daily-image guidance; iii) transposing of the final plan calculated on the CT-sim with 3Dp-mask onto the warped CT to quantify the dosimetric impact of the novel mask material, as this could be relevant downstream during broader implementation of methods and workflows.

In both arms, contouring, dose prescription, dosimetric goals, quality assurance, and daily cone-beam CT (CBCT) image-guidance followed departmental standard-of-care.

2.2. 3D printed mask generation process

MR T1-weighted axial images were imported to Materialise Mimic 18.0 (Materialise NV, Leuven, Belgium). Surface (facial/head) contours were generated using auto threshold with manual delineation where appropriate, allowing the subsequent creation of a 3D mesh. Pixilation of the surface contours was reduced by smoothing and wrapping functions to ensure optimal fitting while preventing discomfort points.

The patient-specific mask was created as an external surface 5–6 mm additament to the facial/head 3D mesh. Given the relative greater thickness of the 3D-printed mask in comparison to the standard T-mask (2 mm), tests were run including ion chamber measurement using a sphere phantom and a 6MV photon beam (Gantry 0°) with and without mask, leading to the optimization of the 3D-p mask density and calculated dose attenuation <1%. In addition, RT plans generated with the mask were transposed to the reciprocal CT image-set with the mask's density overridden to air, showing negligible differences in target and organs-at-risk doses within acceptable tolerance (<1%). Details of the preliminary and supporting data is provided in the Supplementary Materials.

The 3D-printed mask design included full coverage of the posterior portion of the head, while the anterior piece aimed to cover from the nasal bridge-infraorbital rim-zygomatic arch superiorly, encircling eyes and partial forehead in openings. The posterior half of the mask included a standard 'headrest' with three additional attachments that allowed it to be secured directly to the LINAC's couch tabletop. The isocenter was defined in the MR coordinates, roughly at the center of the target volume, allowing to include the surface representation in the 3Dp-mask for daily alignment with the LINAC's isocenter lasers. Subsequently, the mask openings were adjusted to minimize the amount of material on the beam/arc treatment angles. Similarly, the locking blocks between the two mask pieces were configured away and below the coronal plane of the isocenter. A complete 3Dp-mask model is shown in Fig. 1. In addition, 1 mm spacers were created that could be inserted between the locking blocks elements of the two mask pieces, allowing tightening flexibility and adjustments to accommodate soft-tissue variability within the fitting (see Supplementary materials, Figs. S1 and S2).

The finalized 3D-mask model was transferred as a stereolithography (STL) file to the 3D-printer (Stratasys Dimension 1200es; Stratasys, Rehovot, Israel). Printing material included ABSplus or PC-ABS, in respectively lower in-fill or sparse settings to minimize the amount and

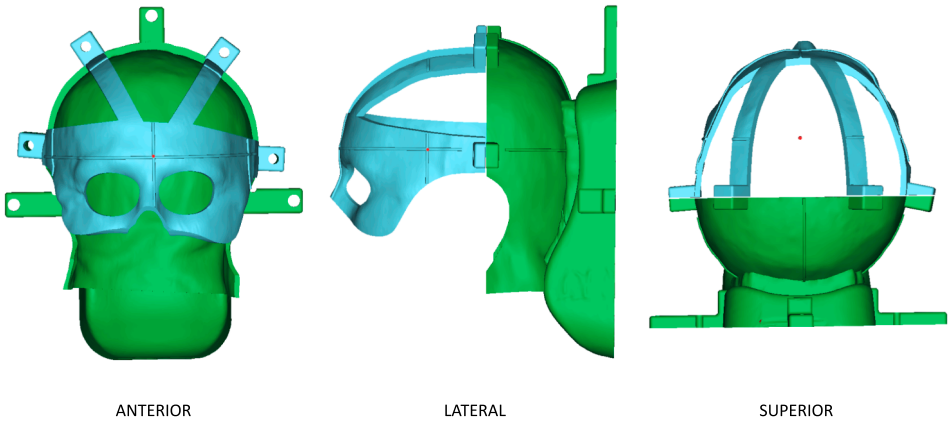

Fig. 1. Final rendering of the 3Dp-mask of a patient in the investigational arm. Views from anterior (left), lateral (central), and superior (right) perspectives are shown. The two parts of the mask are depicted with different colors for illustration purposes only. The red dot in all three views represents the isocenter. Pins (four to attach the 3Dp-mask parts to each other, and three to attach the posterior element of the 3Dp-mask to the LINAC tabletop) are not shown. (For interpretation of the references to colour in this figure legend, the reader is referred to the web version of this article.)

density of material in the 3Dp-mask. After printing completion, the two mask pieces were immersed in a cleaning station for approximately 24 h to remove any dissolvable printing-support elements.

2.3. Technical and clinical evaluations

Prior to each RT session, patients were positioned and aligned based on the in-room lasers and surface marks on the T- or 3Dp-mask. CBCT was obtained and rigidly registered (i.e., bony match) to the CT-sim. Required translational adjustments on positioning through couch shifting were quantified and recorded prospectively.

Patients were assessed for side-effects on a weekly basis during RT by their treating physician as per standard-of-care. Patient-reported adverse events and tolerability of the immobilization system were conducted at predefined time points: i) control arm: after CT-sim, and after a treatment session during first and last weeks of RT with T-mask; ii) investigational arm: after each CT-sim session (i.e., T-mask and 3Dp-mask), after a treatment session during the end of the first and last weeks of RT with 3Dp-mask, and after treatment completion and being immobilized for 10 min with their original T-mask.. The questionnaire consisted of a total of 7 questions (see Supplementary Materials), rating the overall impression during the mask setup procedure (Q1) and during the delivery of the treatment (Q3) with a 5-point Likert scale (*very good, good, fair, poor, very poor*); and the overall discomfort during the mask setup procedure (Q2), the delivery of the treatment (Q4), as well as the specific discomfort in the face (Q5), neck (Q6) and shoulders (Q7) during the treatment delivery with a 6-point Likert scale (*no discomfort, mild, discomforting, distressing, horrible, excruciating*).

2.4. Statistical analyses

Descriptive statistics were used to summarize patient characteristics, RT plan dosimetric indices, and inter-fraction displacement shifts in the investigational and control arms. Dosimetric comparisons between delivered and transposed plans were done using paired *t*-test and Gamma index pass rates. Comparison of CBCT-quantified shift data and couch adjustment displacement values between control and investigational arms was done using independent *t*-test. Unadjusted Wilcoxon signed rank test was used to compare item ratings between investigational and control groups which were carried out independently for each time point to assess any cross-sectional differences. Paired Wilcoxon signed rank tests were performed for the comparison of the ratings for the T-mask and 3Dp-mask within the investigational group at the end of the last RT week. All tests were performed two-sided; p-values < 0.05 were deemed significant. All statistical analyses were performed using R (version 4.1.0).

3. Results

3.1. Patient characteristics

Between January 2020 and July 2022, a total of 40 patients were enrolled (20 per arm), all completing RT and per protocol evaluations. Patient characteristics are shown in Table 1.

3.2. RT planning and delivery

Median RT dose and fractions were 54 Gy (range 20–60) and 30 (range 5–30), respectively. Median time from simulation to ready-to-treatment was 4 days (range 1–12) and 8 days (range 6–14) for the control and investigational arms, respectively. Of note, for the purposes of this proof-of-concept study the processes (i.e., MR/CT-Sim, moulding, 3Dp-mask generation and printing, RT planning) were largely sequential and the investigational arm had an additional CT-Sim (i.e., with the 3Dp-mask), therefore these results may not reflect a future parallel workflow. The average time to complete the 3Dp-mask design and printing was 36 h 50 min (range 12 h 56 min – 42 h 01 min).

3.3. Dosimetric indices

We included a dosimetric quantification which was not required for the patients in study, but pertinent to the proposed paradigm. Statistically significant differences were observed across targets and OARs, albeit of small magnitude (average dose difference of up to 1.59% between delivered and transposed plan; Supplementary Materials, Table S1 and Fig. S3). These differences translated into categorical changes in the fulfillment of 6 (4.3%) standard-of-care protocol objectives among 5 patients (see Supplementary Materials, Table S2). Similarly, the pass rate of gamma index (3%/0mm and 2%/0mm) across the relevant volume was greater or equal to 95% in all 20 and 15 cases, respectively (Supplementary Materials, Table S3).

Table 1
Patient characteristics.

	Control Arm (=20)	Investigational Arm (=20)
Age		
Median (range)	53 (20–82)	60.5 (18–79)
Sex		
Male	10	11
Female	10	9
Diagnosis		
CNS glioma	12	11
Brain metastases	5	5
Meningioma	1	5
Craniopharyngioma	2	3
Central neurocytoma	–	1

Table 2
Absolute inter-fraction displacements (cm) for the entire cohort, control, and investigational arms.

	Full Sample (n = 40)	Control Arm (n = 20)	Investigational Arm (n = 20)	p-value
Left/right				0.76
Mean (sd)	0.080 (0.073)	0.077 (0.064)	0.084 (0.083)	
Median (Q1,Q3)	0.052 (0.024, 0.120)	0.052 (0.034, 0.100)	0.049 (0.021, 0.120)	
Range (min, max)	(0.000, 0.280)	(0.000, 0.207)	(0.003, 0.280)	
Anterior/posterior				**0.001**
Mean (sd)	0.151 (0.118)	0.210 (0.126)	0.093 (0.076)	
Median (Q1,Q3)	0.128 (0.062, 0.205)	0.184 (0.125, 0.280)	0.091 (0.033, 0.133)	
Range (min, max)	(0.000, 0.493)	(0.003, 0.493)	(0.000, 0.320)	
Superior/inferior				**0.01**
Mean (sd)	0.150 (0.119)	0.103 (0.075)	0.197 (0.137)	
Median (Q1,Q3)	0.134 (0.051, 0.230)	0.083 (0.040, 0.163)	0.208 (0.082, 0.262)	
Range (min, max)	(0.000, 0.463)	(0.007, 0.248)	(0.000, 0.463)	

3.4. Inter-fraction displacements (CBCT shift data)

The shift data (measured in cm) for the different directions (i.e., left, right, anterior, posterior, superior, and inferior) were overall comparable between study arms (see Supplementary Materials, Table S4 and Fig. S4). The differences in absolute displacements in the left–right, anterior-posterior, and superior-inferior axes are shown in Table 2. There was no significant difference in the mean values for the left–right absolute displacements. However, the anterior-posterior absolute displacement was greater with the T-mask (Investigational group mean [sd] = 0.09 cm[0.08], Control group mean[sd] = 0.21 cm[0.13], Wilcoxon signed rank p = 0.001), while the absolute superior-inferior displacement was larger in the investigational arm (Investigational group mean[sd] = 0.20 cm[0.14], Control group mean[sd] = 0.10 cm [0.08]; Wilcoxon signed rank p = 0.01). Frequency of inter-fraction absolute displacements along the three axes are represented in Fig. 2. Overall, the performance of the investigational immobilization device appeared comparable to the acceptable tolerance for the current standard-of-care, with median deviations within our institutional planning target volume expansions (0.3 cm with daily CBCT image-guidance).

3.5. Patient-reported outcomes (Questionnaire Analysis)

Patient-reported tolerability with the immobilization systems is shown in Table 3. Overall impression and level of comfort at baseline (i.e., after undergoing CT-Sim and moulding session) for the T-mask did not significantly differ between control and investigational arms. However, patients in the investigational arm who underwent fitting of the 3Dp-mask after their second CT-Sim reported significantly lower facial discomfort (question 5; mean[sd] = 1.11[0.32], compared to control arm mean[sd] = 1.40[0.50], p = 0.04), without other significant differences between arms at this time point.

At the end of the first week of RT, the overall impression and level of comfort did not significantly differ between both arms. However, during the last week of RT, the overall level of comfort was significantly better ($p < 0.05$) with the 3Dp-mask in the aspects pertaining to questions 4 to 6 (i.e., time immobilized during treatment in the mask, facial discomfort, and neck discomfort). Finally, during the last week of RT, patients in the investigational arm were re-fitted their original T-mask. The 3Dp-mask compared to the T-mask had significantly better ratings for questions 1 to 6 ($p < 0.05$ for all items).

Patients subjectively reported less pressure and confinement sensation with the 3Dp-mask than with the T-mask (see Supplementary Material). No adverse events were recorded for either immobilization method.

4. Discussion

This prospective proof-of-concept study lays the foundation for a 'total inverse planning' paradigm; in which end-to-end brain RT merely requires an MR imageset. Using additive manufacturing, we created and deployed a 3D-printed immobilization device that recreates and reproducibly immobilizes the random head positioning during MR acquisition. We demonstrated feasibility, robust performance, and better patient-reported outcomes with the 3Dp-mask compared to conventional T-mask. The 'total inverse planning' workflow would have tangible benefits (Fig. 3): i) eliminates the need for moulding session and CT-sim, thus reducing costs and allowing realignment of resources (e.g. human, imaging), ii) streamlines the brain RT pipeline by enabling anticipatory and/or parallel processes (e.g., planning and 3Dp-mask generation could begin before patient consultation), iii) circumvents the need for MR-CT image registration and any uncertainties derived thereof; and iv) improves the patient's experience throughout their brain RT journey.

Previous work has explored the use of additive manufacturing to generate immobilization devices for the head, however almost all these efforts have remained exploratory without reaching the clinical realm [9]. In 2002, Sanghera et al. first showed technical feasibility of facial surface scanning to generate a virtual mask that could be then 3D-printed [10]. In 2014, a team from the UK was able to generate the front part of 'head shells' from DICOM CT and MR imaging data, and studied the dosimetric properties of various printing materials [11]. A reversed method was explored by a group in Montreal who printed head phantoms from CT-sim images, to then mould the traditional T-mask, and showed acceptable setup agreement indices between co-registered CT scans of 3D-printed heads and the original CT-sim of patients undergoing whole-brain RT [12]. To our knowledge, the only previous work reaching the clinical realm, is from the Heidelberg group who initially reported on a 3Dp-mask generated from MR data, and tested its performance in eight healthy-volunteers undergoing repeated MR imaging (e.g., simulating the fractionated RT scenario) [13]. Subsequently, their method was evaluated in a cohort of six patients undergoing whole-brain RT, showing comparable inter-fractional setup accuracy to ten contemporary patients undergoing head and neck RT analyzed retrospectively [14]. Together, this body of work has demonstrated feasibility and favorable performance of various 3D-printing solutions for head positioning and immobilization. Our work uniquely contributes to the literature as it provides: i) demonstration of feasibility in the setting of representative brain RT prescriptions and techniques, ii) prospective evaluation in a registered trial, including *a priori* defined control group, iii) customizable design with uncovered eyes, nose, ear lobes and mouth to help ameliorate already stressful situation for patients, iv) evaluation encompassing dosimetric, set-up accuracy, and patient's experience, and v) practicability in the clinical realm with an explicit value proposition for rethinking the current workflow.

Additive manufacturing properties could be capitalized in the context of our work to further improve the *status quo*. For pediatric patients, thematic designs could be incorporated to the 3Dp-mask as part of patient-centric initiatives aiming to improve the child's experience and reduce need for anesthesia, as has been achieved for diagnostic imaging procedures [15]. Additionally, the proposed 3Dp-mask

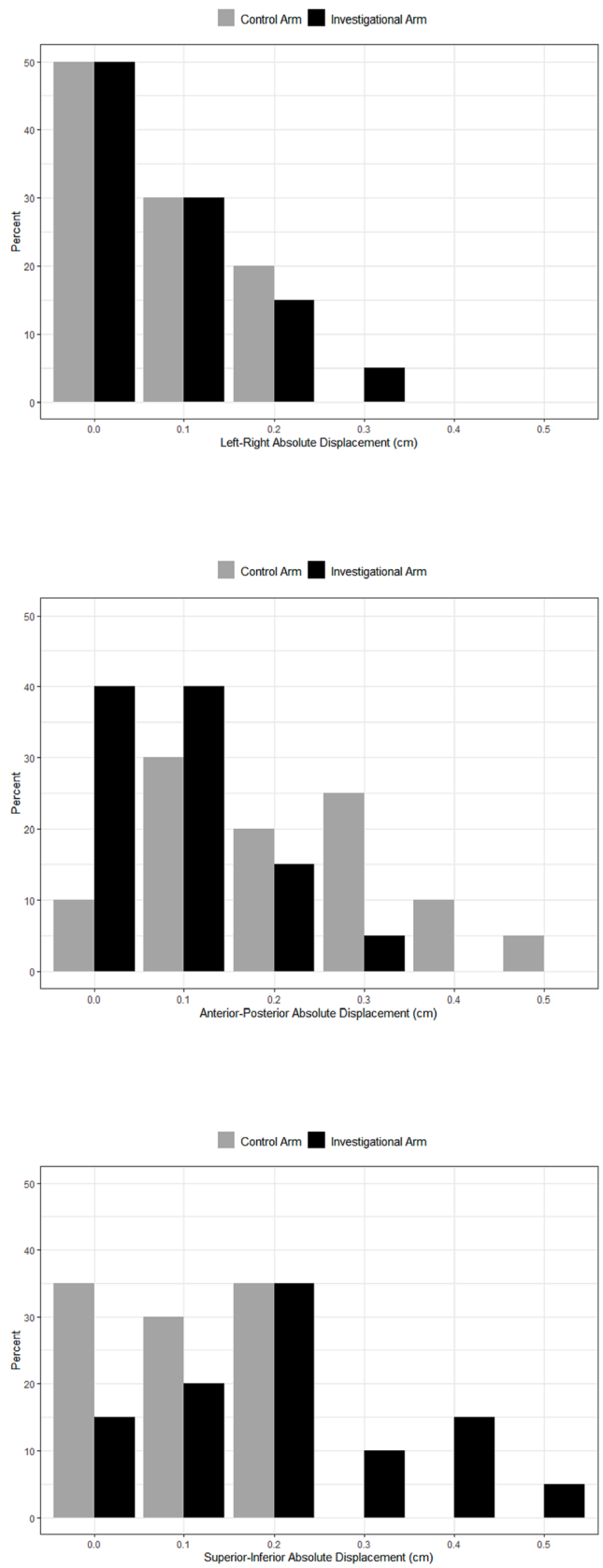

Fig. 2. Frequency histograms of the absolute displacements along the left/right (top), anterior-posterior (middle) and superior-inferior (bottom) axes for the control and investigational arm. Continuous absolute displacements were rounded off to the nearest tenth of a cm so that for example < 0.05="0.0", 0.05 to < 0.15 = "0.1", 0.15 to < 0.25 = "0.2", etc.

approach could be particularly valuable in the head/neck re-treatment setting, whereas positioning could be robustly replicated throughout treatments to maximize cumulative dosimetric certainty for critical structures. In the future, it is foreseeable that additive manufacturing 'shells' could be applied to other body sites with the same goal of recreating reproducible positioning and immobilization from existing image sets. These adaptations should be embraced and encouraged by the predicted increase in availability and use-cases for additive manufacturing, with corresponding drops in costs [4]. In this evolving context, we could speculate different models to access this technology in RT. For example, high-volume centres could house 'end-to-end' solutions on-site, while remote services (i.e., image processing, mask design, 3D printing) could emerge, thus removing barriers both logistically and economically for smaller radiation centres engagement.

This clinical study has some limitations. First, this is a single-institution non-randomized trial. However, it was devised to serve as a proof-of-concept, and randomization would have not removed susceptibility to confounders due to the intervention type and open-label nature. We attempted to maximize arms comparability with uniform RT planning, quality assurance, delivery, and patient-reported endpoints; the latter including ascertainment during T-mask moulding and CT-sim for all patients, and repeated fitting of T-mask at the end of treatment in the investigational arm. Secondly, the observation period in this study is short, and does not include oncologic outcomes. However, considering the objectives of this study, we had no *a priori* justification for evaluation beyond well-established surrogates (e.g., dosimetric constraints) and/or follow-up after RT delivery completion. Thirdly, we established the feasibility of an MR-only 'total inverse planning', however patients in this study underwent CT-sim and moulding session, and their RT plans were calculated based on CT-derived tissue densities. MR-based planning with inferred densities (i.e., synthetic CT) has been previously shown to be safe and accurate [16], and was not a primary objective of this work. Furthermore, given the nature of this study, having a judicious fallback option (e.g., CT-sim and T-mask in all patients) was deemed essential. In a similar vein, we did observe a quantifiable dosimetric impact of the 3Dp-mask, albeit of low magnitude and questionable clinical relevance. Thus, in an MR-only paradigm, additional work may be required to identify cases more susceptible to dose variations between planned (e.g., without mask) vs delivered (e.g., with mask), or methods to account and/or compensate for the expected attenuation introduced by the mask's material (e.g., integrating the STL files onto the DICOM RT structures within the TPS; importing the first CBCT for dose re-calculation). Last, the 3Dp-mask method did not seek to maximize direct costs savings. Additional work might be required to optimize its design, in turn decreasing printing material and time. In a similar vein, the 3Dp-mask design allowed for the use of 1 mm spacers that 'expanded' the mask internal volume thus introducing degrees of freedom to account for changes in anatomy (e.g., facial swelling with use of steroids) aiming to improve patients' comfort and experience while retaining a tight fitting more similar to the baseline. It should be acknowledged though that this system could introduce an operator dependent feature. However, the use of spacers due to facial swelling was only required for 2 subjects in the present study, for a limited number of fractions (towards the end of the RT treatment) and the treatment delivery was ultimately based on the CBCT registration to match the bony anatomy.

5. Conclusion

Design of novel immobilization devices using additive manufacturing may provide a comparable inter-fraction performance to conventional immobilization masks for CNS RT, while offering better patient-reported experience. This works lays the foundation for a 'total inverse planning' paradigm whereby all RT planning and delivery processes stem solely from a single MR image-set, circumventing the need for additional or redundant planning imaging studies. Towards the goal

Table 3
Patient-reported tolerability of the immobilization systems across pre-defined timepoints. (A) Comparison between the investigational arm (3Dp-mask) and the control arm (T-mask). (B) Fitting of the T-mask in the investigational arm patients and comparison to the control arm.

A.

	Post CT-Sim			**End of 1st RT Week**			**End of last RT Week**		
	Control (T-mask, n=20)	Investigational (3Dp-mask, n=20)	p-value	Control (T-mask, n=20)	Investigational (3Dp-mask, n=20)	p-value	Control (T-mask, n=20)	Investigational (3Dp-mask, n=20)	p-value
Q1: overall impression of the mask setup procedure			0.31			0.81			0.54
Mean (sd)	1.30 (0.47)	1.16 (0.37)		1.28 (0.46)	1.32 (0.67)		1.33 (0.59)	1.20 (0.41)	
Median (Min,Max)	1 (1, 2)	1 (1, 2)		1 (1, 2)	1 (1, 3)		1 (1, 3)	1 (1, 2)	
Missing	0	1		2	1		2	0	
Q2: overall discomfort during the mask setup procedure			0.49			0.91			0.08
Mean (sd)	1.35 (0.59)	1.21 (0.42)		1.33 (0.59)	1.32 (0.48)		1.50 (0.99)	1.10 (0.31)	
Median (Min,Max)	1 (1, 3)	1 (1, 2)		1 (1, 3)	1 (1, 2)		1 (1, 5)	1 (1, 2)	
Missing	0	1		2	1		2	0	
Q3: overall impression during the time that you were immobilized (e.g during treatment) in the mask			0.11			0.55			0.32
Mean (sd)	1.50 (0.61)	1.21 (0.42)		1.44 (0.62)	1.42 (0.84)		1.56 (0.78)	1.30 (0.47)	
Median (Min,Max)	1 (1, 3)	1 (1, 2)		1 (1, 3)	1 (1, 4)		1 (1, 4)	1 (1, 2)	
Missing	0	1		2	1		2	0	
Q4: your overall discomfort during the time that you were immobilized (e.g. during treatment) in the mask			0.22			0.42			**0.005**
Mean (sd)	1.20 (0.41)	1.21 (0.92)		1.33 (0.59)	1.21 (0.54)		1.61 (0.98)	1.05 (0.22)	
Median (Min,Max)	1 (1, 2)	1 (1, 5)		1 (1, 3)	1 (1, 3)		1 (1, 5)	1 (1, 2)	
Missing	0	1		2	1		2	0	
Q5: discomfort on your face during treatment			**0.04**			0.49			**0.006**
Mean (sd)	1.40 (0.50)	1.11 (0.32)		1.33 (0.59)	1.26 (0.65)		1.33 (0.49)	1.00 (0.00)	
Median (Min,Max)	1 (1, 2)	1 (1, 2)		1 (1, 3)	1 (1, 3)		1 (1, 2)	1 (1, 1)	
Missing	0	1		2	1		2	0	
Q6: discomfort in your neck during treatment			0.32			0.98			**0.03**
Mean (sd)	1.20 (0.52)	1.05 (0.23)		1.11 (0.32)	1.11 (0.32)		1.28 (0.57)	1.00 (0.00)	
Median (Min,Max)	1 (1, 3)	1 (1, 2)		1 (1, 2)	1 (1, 2)		1 (1, 3)	1 (1, 1)	
Missing	0	1		2	1		2	0	
Q7: discomfort in your shoulders during treatment			0.17			0.33			0.06
Mean (sd)	1.10 (0.31)	1.00 (0.00)		1.06 (0.24)	1.00 (0.00)		1.17 (0.38)	1.00 (0.00)	
Median (Min,Max)	1 (1, 2)	1 (1, 1)		1 (1, 2)	1 (1, 1)		1 (1, 2)	1 (1, 1)	
Missing	0	1		2	1		2	0	

Q1, Q3 – 1: very good; 2: good; 3: fair; 4: poor; 5: very poor
Q2, Q4-Q7 – 1: no discomfort; 2: mild; 3: discomforting; 4: distressing; 5: horrible; 6: excruciating

B.

	Post CT-Sim		**End of last RT Week**	
	Investigational (T-mask, n=20)	p-value	Investigational (T-mask, n=20)	p-value
Q1: overall impression of the mask setup procedure		0.46		**<0.001**
Mean (sd)	1.45 (0.60)		2.35 (0.86)	
Median (Min,Max)	1 (1, 3)		2 (1, 4)	
Missing	0		3	
Q2: overall discomfort during the mask setup procedure		0.1		**0.02**
Mean (sd)	1.75 (0.85)		1.82 (0.53)	
Median (Min,Max)	2 (1, 4)		2 (1, 3)	
Missing	0		3	
Q3: overall impression during the time that you were immobilized (e.g during treatment) in the mask		0.8		**<0.001**
Mean (sd)	1.60 (0.75)		2.65 (0.86)	
Median (Min,Max)	1 (1, 3)		3 (1, 4)	
Missing	0		3	
Q4: your overall discomfort during the time that you were immobilized (e.g. during treatment) in the mask		0.25		**0.01**
Mean (sd)	1.45 (0.69)		2.06 (0.56)	
Median (Min,Max)	1 (1, 3)		2 (1, 3)	
Missing	0		3	
Q5: discomfort on your face during treatment		0.48		**0.02**
Mean (sd)	1.35 (0.67)		1.82 (0.64)	
Median (Min,Max)	1 (1, 3)		2 (1, 3)	

(*continued on next page*)

Table 3 (*continued*)

B.	Post CT-Sim		End of last RT Week	
	Investigational (T-mask, n=20)	p-value	Investigational (T-mask, n=20)	p-value
Missing	0		3	
Q6: discomfort in your neck during treatment		0.4		0.08
Mean (sd)	1.40 (0.75)		1.65 (0.70)	
Median (Min,Max)	1 (1, 3)		2 (1, 3)	
Missing	0		3	
Q7: discomfort in your shoulders during treatment		0.16		0.34
Mean (sd)	1.00 (0.00)		1.06 (0.24)	
Median (Min,Max)	1 (1, 1)		1 (1, 2)	
Missing	0		3	
Q1, Q3 – 1: very good; 2: good; 3: fair; 4: poor; 5: very poor				
Q2, Q4-Q7 – 1: no discomfort; 2: mild; 3: discomforting; 4: distressing; 5: horrible; 6: excruciating				
P-values)unadjusted Wilcoxon signed rank test) resultant from comparison to control arm at the corresponding timepoints				

Abbreviations: CT, computed tomography; RT, radiotherapy; T-mask, thermoplastic mask; 3Dp-mask, 3D printed mask; Q, question; sd, standard deviation. P-values are resultant from unadjusted Wilcoxon signed rank test comparing responses between investigational and control arms at each of the corresponding time points. P value < 0.05 was considered statistically significant.

of MR-only treatments, further efforts should be undertaken in this direction to materialize improvements in RT workflows and save costs.

Funding

This study received funding from an Adam Coules Research Grant from the Patient & Family Advisory Committee (PFAC) of The Gerry & Nancy Pencer Brain Tumor Centre at Princess Margaret Cancer Centre, and the Princess Margaret Cancer Foundation. Guided Therapeutics (GTx) program is supported by the P. Austin Family Foundation Guided Therapeutics International Fellowship Fund, the Dorrance Drummond Family Fund, the Garron Foundation, the Strobele Family Guided Therapeutics Research Fund and the Kevin and Sandra Sullivan Chair in Surgical Oncology. Funding bodies had no role in design and conduct of the study; collection, management, analysis, and interpretation of the data; and preparation, review, or approval of the manuscript.

Data sharing agreement

Deidentified participant data from this trial will be shared upon request with appropriate Data Sharing Agreements in place.

CRediT authorship contribution statement

Paola Anna Jablonska: Investigation, Data curation, Writing – original draft, Writing – review & editing, Project administration, Visualization. **Amy Parent:** Methodology, Validation, Formal analysis, Writing – review & editing. **Nancy La Macchia:** Methodology,

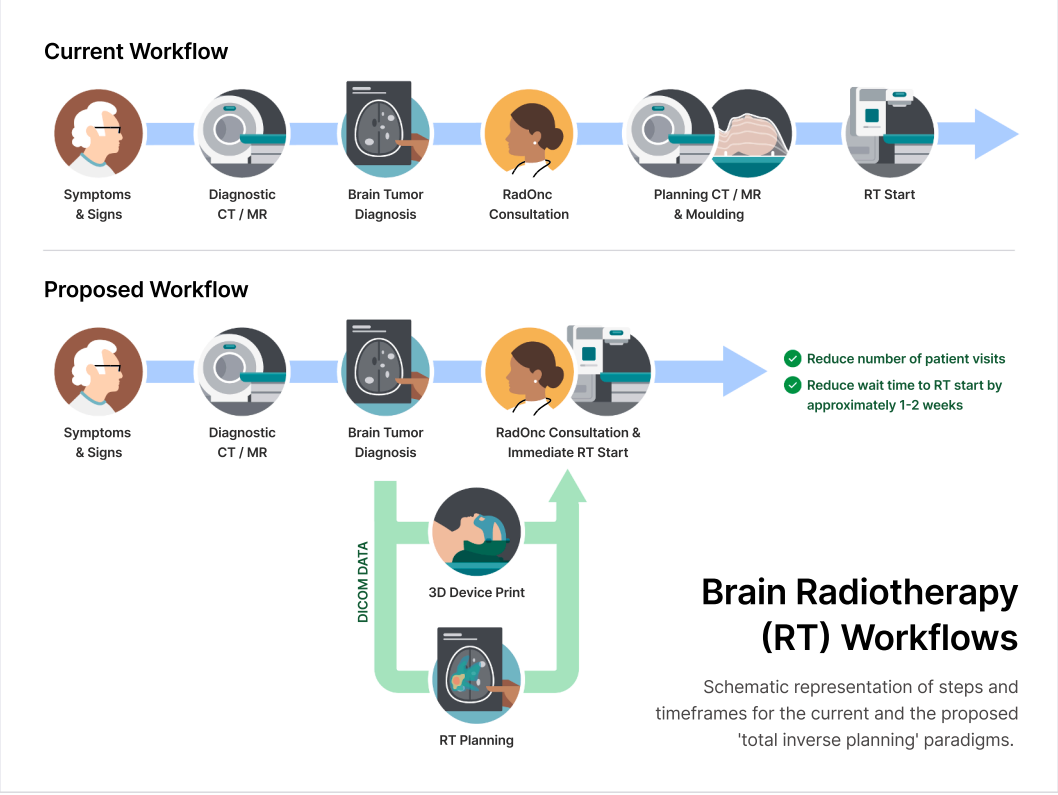

Fig. 3. Brain radiotherapy (RT) workflows. Schematic representation of steps and timeframes for the current and the proposed 'total inverse planning' paradigms. Abbreviations: CT, computed tomography; MR, magnetic resonance; RadOnc, radiation oncologist; 3D, three-dimensional.

Validation, Formal analysis, Writing – review & editing. **Harley H.L. Chan:** Conceptualization, Methodology, Software, Formal analysis, Resources, Writing – review & editing, Visualization. **Matthew Filleti:** Methodology, Resources. **Matthew Ramotar:** Data curation, Methodology, Resources, Writing – review & editing. **Young-Bin Cho:** Methodology. **Maria Braganza:** Investigation, Data curation, Project administration. **Adam Badzynski:** Visualization. **Normand Laperriere:** Investigation, Writing – review & editing. **Tatiana Conrad:** Investigation, Writing – review & editing. **Derek S. Tsang:** Investigation, Writing – review & editing. **David Shultz:** Investigation, Writing – review & editing. **Anna Santiago:** Formal analysis. **Jonathan C. Irish:** Methodology, Resources, Funding acquisition. **Barbara-Ann Millar:** Investigation, Writing – review & editing. **Tony Tadic:** Methodology, Resources, Writing – review & editing, Supervision. **Alejandro Berlin:** Conceptualization, Investigation, Writing – original draft, Writing – review & editing, Visualization, Supervision, Project administration, Funding acquisition.

Declaration of Competing Interest

The authors declare that they have no known competing financial interests or personal relationships that could have appeared to influence the work reported in this paper.

Appendix A. Supplementary data

Supplementary data to this article can be found online at https://doi.org/10.1016/j.ctro.2023.100663.

References

[1] Lamba N, Wen PY, Aizer AA. Epidemiology of brain metastases and leptomeningeal disease. Neuro-Oncol 2021;23:1447–56.
[2] Jonsson J, Nyholm T, Söderkvist K. The rationale for MR-only treatment planning for external radiotherapy. Clin Transl Radiat Oncol 2019;18:60–5.
[3] D'Aveni R. The 3-D Printing Revolution. Harv Bus Rev 2015.
[4] Liaw C-Y, Guvendiren M. Current and emerging applications of 3D printing in medicine. Biofabrication 2017;9(2):024102.
[5] Wang X, Wang X, Xiang Z, et al. The Clinical Application of 3D-Printed Boluses in Superficial Tumor Radiotherapy. Front Oncol 2021;11:698773.
[6] Held T, Herpel C, Schwindling FS, et al. 3D-printed individualized tooth-borne tissue retraction devices compared to conventional dental splints for head and neck cancer radiotherapy: a randomized controlled trial. Radiat Oncol Lond Engl 2021;16:75.
[7] Song WY, Robar JL, Morén B, Larsson T, Carlsson Tedgren Å, Jia X. Emerging technologies in brachytherapy. Phys Med Biol 2021;66(23):23TR01.
[8] Nixon JL, Brown B, Pigott AE, et al. A prospective examination of mask anxiety during radiotherapy for head and neck cancer and patient perceptions of management strategies. J Med Radiat Sci 2019;66:184–90.
[9] Asfia A, Novak JI, Mohammed MI, et al. A review of 3D printed patient specific immobilisation devices in radiotherapy. Phys Imaging Radiat Oncol 2020;13:30–5.
[10] Sanghera B, Amis A, McGurk M. Preliminary study of potential for rapid prototype and surface scanned radiotherapy facemask production technique. J Med Eng Technol 2002;26:16–21.
[11] Laycock SD, Hulse M, Scrase CD, et al. Towards the production of radiotherapy treatment shells on 3D printers using data derived from DICOM CT and MRI: preclinical feasibility studies. J Radiother Pract 2015;14:92–8.
[12] Pham Q-VV, Lavallée A-P, Foias A, et al. Radiotherapy Immobilization Mask Molding Through the Use of 3D-Printed Head Models. Technol. Cancer Res. Treat. 2018;17:1533033818809051.
[13] Haefner MF, Giesel FL, Mattke M, Rath D, Wade M, Kuypers J, et al. 3D-Printed masks as a new approach for immobilization in radiotherapy - a study of positioning accuracy. Oncotarget 2018;9(5):6490–8.
[14] Mattke M, Rath D, Häfner MF, et al. Individual 3D-printed fixation masks for radiotherapy: first clinical experiences. Int J Comput Assist Radiol Surg 2021;16:1043–9.
[15] Jaimes C, Gee MS. Strategies to minimize sedation in pediatric body magnetic resonance imaging. Pediatr Radiol 2016;46:916–27.
[16] Paradis E, Cao Y, Lawrence TS, et al. Assessing the Dosimetric Accuracy of Magnetic Resonance-Generated Synthetic CT Images for Focal Brain VMAT Radiation Therapy. Int J Radiat Oncol Biol Phys 2015;93:1154–61.